Integrated Design Results for the MSR DAC-0.0 Mars Ascent Vehicle

Darius Yaghoubi
Mail Stop EV41
4600 Rideout Road
Marshall Space Flight Center, AL 35812
darius.f.yaghoubi@nasa.gov

Peter Ma
Mail Stop EV70
4221 Rideout Road
Marshall Space Flight Center, AL 35812
peter.h.ma@nasa.gov

The NASA Mars Sample Return (MSR) Campaign endeavors to return Martian regolith, rock, and atmospheric samples to Earth for scientific study. One of many significant challenges to overcome in the return of these samples lies in transporting them from the Martian surface to space. In order to surmount this challenge, the Campaign has conceptualized the need for a Mars Ascent Vehicle (MAV) to perform this function and deliver Martian samples to orbit. There, the samples will be ejected and captured by a separate spacecraft for return to Earth.

Many concepts for a MAV have existed in the past, but it has not been until now that an integrated, detailed design solution has been developed and analyzed. Preliminary assessments of the initial architecture examined multiple methods of propulsion. The team ultimately determined that a Two Stage to Orbit (TSTO) solid propulsion vehicle would provide the most effective performance and be the most technologically ready to support this mission. Following the decision to adopt a TSTO solid propelled vehicle, the first official Design Analysis Cycle, DAC-0.0, was performed in Spring 2020 to formally advance the fidelity of the vehicle to a maturity level acceptable for NASA Key Decision Point A (KDP-A).

This paper describes the resultant MAV design concept developed as part of the DAC-0.0 study by the NASA Marshall Space Flight Center (MSFC), in association with the NASA Jet Propulsion Laboratory (JPL). The TSTO vehicle features two solid rocket motors, one powering each stage. Their thrust vectors are controlled with Thrust Vector Control (TVC) systems consisting of independent electromechanical actuators acting on gimballed nozzles. The vehicle is designed to deliver up to 0.47kg of Martian samples to a Mars circular orbit of 343km at 27° inclination. Due to the unique environmental conditions that this vehicle is required to operate in, the subsystem design teams were compelled to develop creative and unorthodox designs to ensure a successful mission. The detailed design and analysis of these subsystems are discussed in this paper and include topics on the MAV Guidance, Navigation, and Control (GNC); structures and mechanisms; integrated vehicle thermal; avionics and flight software; a hydrazine-based Reaction Control System (RCS); aerosciences; and vehicle assembly, integration, and test (AI&T) considerations, among others.

Following the conclusion of the MAV DAC-0.0, additional alternative architecture concepts were also studied to further reduce the mass of the overall system.

TABLE OF CONTENTS

1. INTRODUCTION

The concept of a Mars Ascent Vehicle (MAV) has been studied to varying levels of fidelity since the 1970s. Although many different iterations of a MAV have existed in the past, each with different design constraints and mission concepts, they all have a similar ultimate objective: deliver a payload from the surface of Mars into space. The current MAV design, being developed by NASA Marshall Space Flight Center (MSFC) in association with NASA Jet Propulsion Laboratory (JPL), is part of a larger Mars Sample Return (MSR) campaign. The primary objective of this campaign is to return geological and atmospheric samples from Mars to Earth for study. Despite the advanced robotics technology present in rovers such as Curiosity and Perseverance, their on-board remote laboratories have yet to parallel the advanced capabilities of human-run laboratories here on Earth. The MAV element of the campaign is thus being designed to facilitate this capability, whose specific role is to transport these samples from the Martian surface into Mars orbit.

The first leg of the MSR campaign began in July 2020 with the launch of the Perseverance rover. Once it has landed on the Martian surface, Perseverance will use a robotic drill to collect surface and atmospheric samples from the surface of the Jezero Crater on Mars. These samples will be stored in sample tubes and cached on the surface. In 2026, MAV will be stowed within the Sample Retrieval Lander (SRL) and launched from Earth. After approximately 33 months in interplanetary space, the SRL will land at the Jezero Crater and deploy the Sample Fetch Rover (SFR). The SFR will conduct excursions on the Mars surface to collect the sample tubes left behind by Perseverance and return them to the SRL. Onboard the SRL will be the Sample Transfer Arm (STA). This will move the sample tubes from the SFR and place them into the Orbiting Sample (OS): the payload compartment on the forward end of the MAV. The OS itself will be contained within a MAV Payload Assembly (MPA). The OS will be designed to hold up to 30 sample tubes. Following delivery of sample tubes into the OS, the MAV will be ejected from the SRL and begin its ascent flight to orbit. After achieving the desired target orbit, the MAV will eject the OS, to be captured by a separate Earth Return Orbiter (ERO) and returned to Earth.

The MAV design concept is a two stage, solid rocket motor-propelled vehicle. It features an electromechanically actuated Thrust Vector Control (TVC) system on each stage, a monopropellant Reaction Control System (RCS) with an orbital trim capability, and pyrotechnic stage separation. Combined with the MPA and OS, the entire assembly creates the Mars Ascent System (MAS). A deconstructed view of the DAC-0.0 exit configuration MAS is shown in Figure 1.

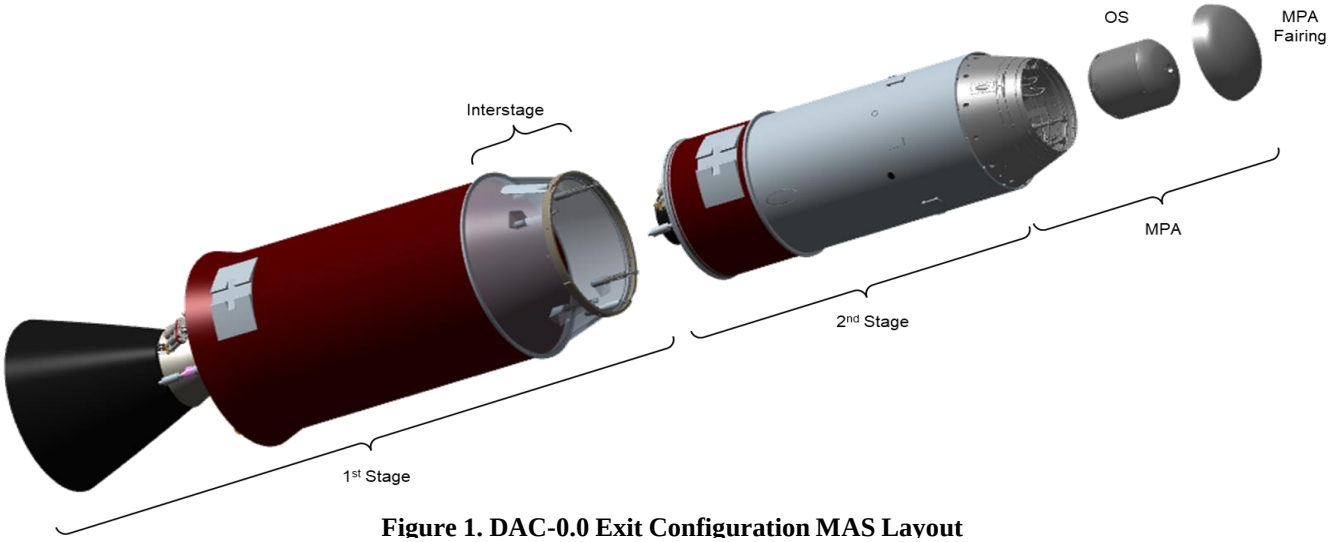

Figure 1. DAC-0.0 Exit Configuration MAS Layout

2. DESIGN ANALYSIS CYCLE-0.0

In the Spring of 2020, NASA MSFC completed the first official Design Analysis Cycle (DAC) for the MAV, DAC-0.0. The primary purpose of this DAC was to advance the fidelity of the vehicle design to a level of maturity acceptable for NASA Key Decision Point A (KDP-A). This transitioned the MAV project from a pre-Phase A design – marked by feasibility concept studies – to a Phase A design defined primarily by concept and technology development. Prior to DAC-0.0, alternative concept configurations were examined. In 2019, a Preliminary Architecture Assessment (PAA) was completed to determine whether a solid[1] or a hybrid[2] propulsion system would be most effective for this mission. Culminating in a Decision Package, the present solid concept was chosen going forward.

Although the ultimate goal of the MAV is to deliver geological and atmospheric samples to Martian orbit, there were several additional driving constraints and requirements to be considered in order to ensure success of the MSR mission. These driving requirements set the Ground Rules and Assumptions (GRAs) for DAC-0.0. Major GRAs include the following: launch from Earth in 2026 to facilitate return of Martian samples in 2031; a project Risk Class B+[3] designation; and a maximum MAV target Gross Liftoff Mass (GLOM) of 525kg with a geometric length not to exceed 3.0m and a diameter not to exceed 0.57m (excluding aft aerodynamic ramp). The payload was defined as the total injected mass at target Mars orbit. This includes the MPA, OS, and Martian samples. For DAC-0.0, the payload total mass was limited to 16kg, including 30 sample tubes. Finally, a set of orbit constraints defined the variation permitted in final orbit insertion. These included a lower bound periapsis of 300km, a semi-major axis variation of ±27km, an inclination angle of 27° ± 0.83°, and a Right Ascension of the Ascending Node (RAAN) variation of ±2.5°.

For DAC-0.0, the flight ascent mission of the MAV begins with ejection from the SRL via a Vertical Egress Controlled TipOff Rate (VECTOR) launch mechanism. This ensures a complete mechanical separation between the SRL and MAV during first stage ignition, shown in Figure 2. Following ejection, the first stage Solid Rocket Motor (SRM1) ignites and burns for approximately 80sec. Following SRM1 burnout, the MAV remains in a coast period for approximately 500sec. During this time, the MPA aerodynamic fairing and entire first stage will separate from the vehicle. After coast, the second stage SRM, SRM2, will

ignite and burn for approximately 20sec, raising the periapsis and circularizing the orbit. Following SRM2 burnout, a third orbital trim burn is performed via axial Orbital Trim Thrusters (OTT) to fine-tune its final orbit parameters. Once the target orbit has been achieved, the MAV will command the MPA to eject the OS, with the latter to be collected by the ERO. This paper hereafter describes the individual subsystems associated with the DAC-0.0 MAV design.

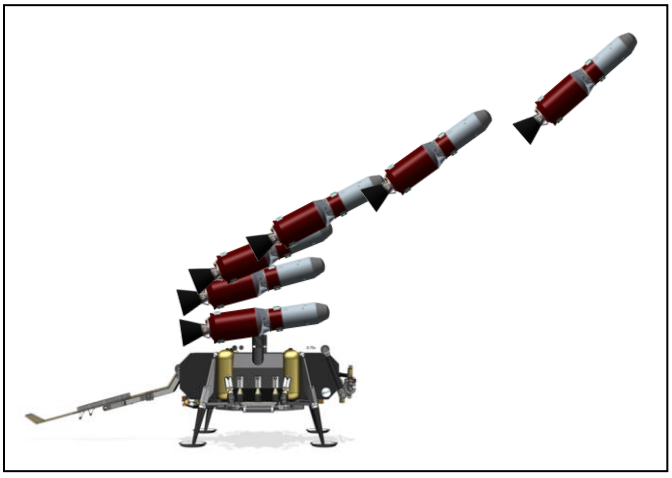

Figure 2. Conceptual VECTOR Launch Methodology

3. MAIN PROPULSION

The MAV main propulsion system consists of two solid rocket motors, each providing axial thrust to inject the Martian samples into orbit. Each SRM has a composite case, a trapped ball nozzle with a supersonic split line, and an electromechanically actuated TVC system providing pitch and yaw control during ascent. Although the integrated design is considered at a mid-level Technology Readiness Level (TRL), the component heritage is fairly high TRL. It has been flight proven in similar environments.

Solid Rocket Motor Design

Initial sizing and optimization of the SRMs began with designs from the previous PAA model. DAC-0.0 GRAs saw an increased GLOM of 525kg, requiring larger SRMs. A new overall case and propellant grain design was developed following maturation of the MAV mass properties, preliminary Guidance, Navigation, and Control (GNC) parameters, aerodynamic databases, and structural/thermal concept design. Additional developments enabled greater performance through optimization of non-propulsion inert mass and case design. Although the study began with a traditional composite cylindrical first stage and spherical titanium second stage SRM, it was later found that a "flattened" composite second stage motor provided an increased dry mass margin and allowed for simpler Assembly, Integration, and Testing (AI&T).

The motors themselves feature TP-H-3062 solid propellant. Earlier studies showed that its Carboxy Terminated Polybutadiene (CTPB) binder was very capable in various extreme temperature ranges. Additionally, it has significant heritage, having operated in Martian environments for both Mars Exploration Rovers Spirit and Opportunity and Mars Pathfinder during Entry-Descent-Landing (EDL). Specific impulse for both SRMs were calculated based upon propellant parameters and nozzle geometry. Ultimately, SRM1 featured 320kg of propellant, while SRM2 featured 49kg of propellant. Figure 3 shows the general shape of each SRM.

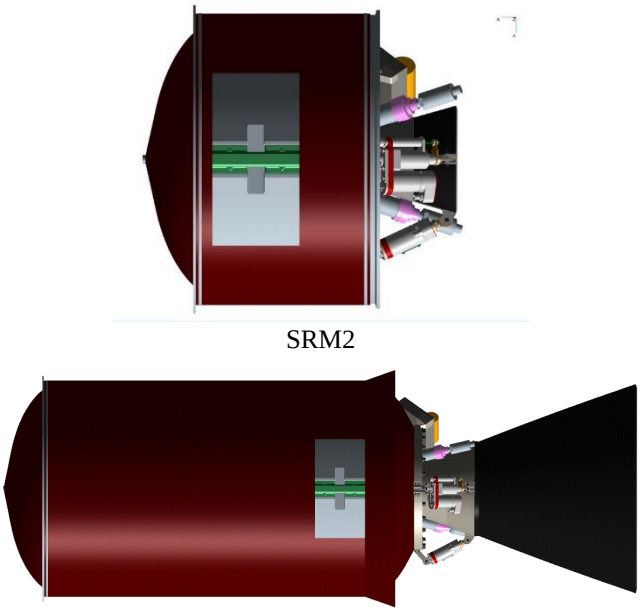

Figure 3. Solid Rocket Motor Shapes

A fluid dynamics analysis was performed to refine SRM nozzle designs and understanding of TVC performance, given the integrated loads induced on the nozzle structure during ascent. In this design, the nozzle gimbal joints feature a SuperSonic Splitline (SSSL), described further in Section 5. Computational Fluid Dynamics (CFD) simulations were completed for both SRMs with aft nozzles positioned at static gimbal angles with varying SSSL gap widths. From here, side force and axial force vectors were calculated aft of the nozzle gimbal, as shown in Figure 4.

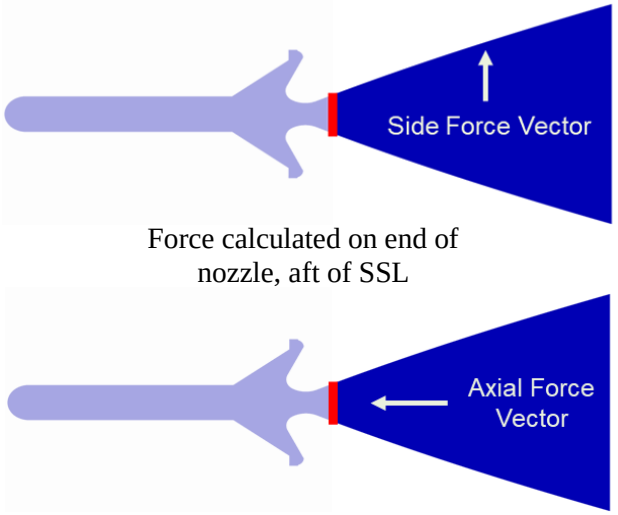

Figure 4. Nozzle Force Vectors

The effect of the SSSL gap was found to be small, less than 1.6% difference between options on aft nozzle forces.

CFD results were also used to refine the initial TVC model by providing fluid-induced nozzle loads. Analysis results were provided as inputs for use in separate TVC sizing and structural dynamics analyses. This study found that transient gimballing simulations matched the static simulations well and did not indicate a non-linear dynamic gimbal response. Dispersions in amplification factor observed at low gimbal angles behaved in a similar manner.

Propulsion Thermal

A thermal assessment was performed on the SRMs and their components to determine the effects of asymmetrical motor heating and internal insulation. Prior to motor ignition, the SRMs will be exposed to extremely low temperatures for long durations. Three heaters were employed on SRM1 in order to maintain a consistent operational Allowable Flight Temperature (AFT) range of -25°C to -15°C. The locations of these heaters and their power level is shown in Figure 5.

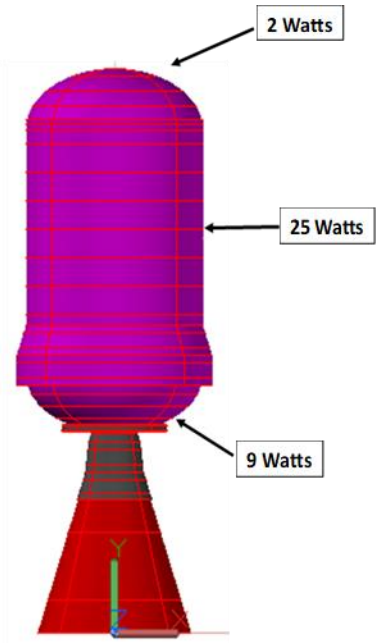

Figure 5. SRM1 Heater Locations

The asymmetrical motor heating analysis found that a maximum temperature gradient of approximately 8°C occurred 225min after being commanded to heat to operational AFT. Although not the intent of the study, it was found that heater powers may need to be more evenly distributed to avoid constant heater cycling.

An evaluation of the internal insulation design was performed to determine Material Decomposition Depths (MDDs) and Actual Factors of Safety (ASFs) at forty axial locations from the forward to aft domes of SRM1. All axial locations were exposed to different average pressures and different exposure times. Thermal analyses were performed for insulation material using Aerotherm Chemical Equilibrium[4] code, the Bartz equation, and the Insulation Thermal Response and Ablation Code[5] code to predict MDDs. The ASFs were calculated from MDDs and pre-fire insulation thickness. The analyses found that ASFs were above 1.5 at all locations of MAV SRM1 motor and the current insulation design thickness is adequate.

Propulsion Loads

One of the unique aspects of the MAV design is its interface with the SRL. Unlike typical launch vehicles that experience maximum loads in the axial direction, the MAV experiences maximum loads in a lateral direction during Mars EDL. The primary load path during this phase must pass directly through the two SRM cases, as they are structurally load bearing and attach directly to the SRL via four attach hard points on the VECTOR, shown in Figure 6.

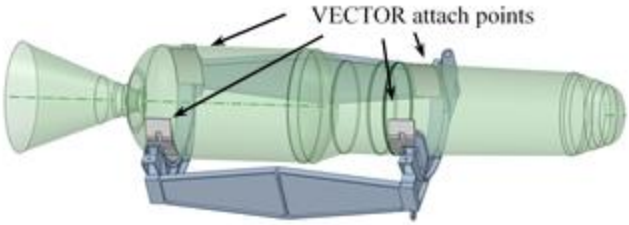

Figure 6. SRL-MAV VECTOR Support Cradle

An analysis on the locations of these attach points compared peak principle and shear stress in the SRM cases. Peak deflection was found to vary by less than 1% between cases, with stress values differing by up to 4%.

In addition to analysis of the hardpoint load paths, general deflection of propulsion hardware was necessary. Initial analysis of the EDL induced loads on the MAV indicated that although the resulting stresses were non-negligible upon the SRM1 nozzle, they were feasibly contained with the current materials. Structure deflection of the SRM nozzles was found to not induce contact between the MAV and SRL. Worst-case stresses occurred during a 15G EDL entry/deceleration step, shown in Figure 7 (deflection exaggerated x5 for clarity). Mechanically locking the TVC system during this phase of the mission would be a viable solution for reducing this deflection.

Figure 7. Deflection of SRM1 Nozzle During EDL

4. REACTION CONTROL SYSTEM

The MAV RCS provides attitude control about the roll axis during motor burns, and full 3-axis control during coast. It consists of a traditional 2-to-1 blowdown monopropellant architecture. The system design will leverage existing high TRL Commercial-Off-The-Shelf (COTS) hardware with delta qualification on most components. A trade study was

performed during DAC-0.0 to assess the optimal type of propellant for use in the RCS. Compared against green propellant and a solid gas generator, hydrazine was chosen due to its high TRL, lower mass, and better contribution to orbital insertion accuracy. In addition to the RCS propellant tank itself, located forward of SRM2 and aft of the avionics plate, the MAV RCS features six lateral thrusters and two axial Orbital Trim Thrusters (OTT). The lateral thrusters were assumed to be Aerojet Rocketdyne MR-111C thrusters, providing up to 5N of lateral thrust each. The OTTs were assumed to be Aerojet Rocketdyne MR-106L thrusters, providing up to 22N of axial thrust each[10]. Actual thrusters used in the final design may vary. The overall layout of the RCS and its location within the second stage are shown in Figure 8.

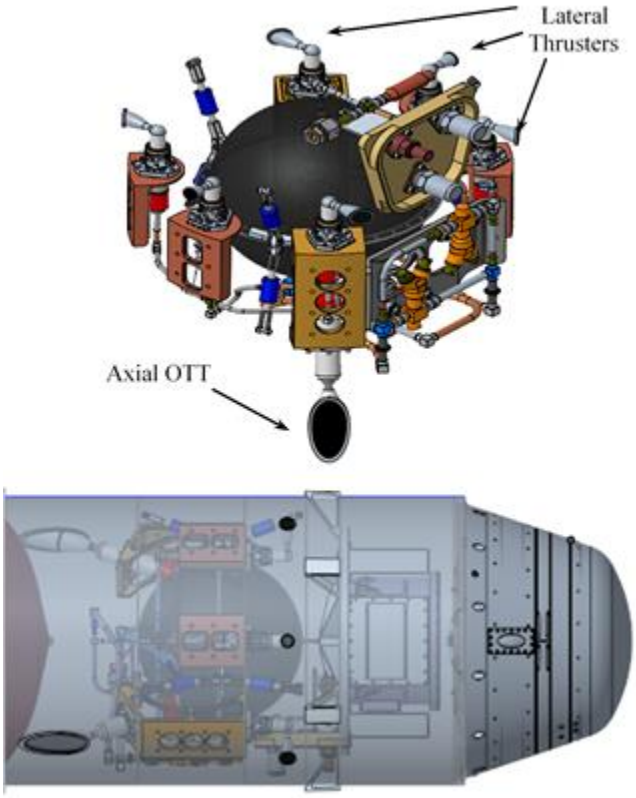

Figure 8. RCS Location and Layout

One of the unique design features of the MAV RCS is the axial OTTs. Due to the inherent nature of solid rocket motors, the propulsion system is unable to actively throttle and shutdown each motor. This would ultimately lead to imprecision in final orbit insertion. To mitigate this, two OTTs were introduced. These act like a third liquid stage of the vehicle, using residual RCS propellant after second stage burnout to increase orbital accuracy. The capability of the OTTs to improve orbital accuracy is discussed in more detail in Section 10.

The RCS propellant is stored in a titanium tank with an elastomeric diaphragm. The diaphragm allows for a minimized ullage within the tank, reducing propellant slosh. Gaseous nitrogen is used as the blowdown pressurant. One downside of using hydrazine as the propellant is its relatively high freezing point. Hydrazine freezes at 2°C, which is a substantially higher temperature than the vehicle non-operational minimum AFT of -40°C. This necessitates specialized heaters for the wetted RCS components to ensure that they do not freeze. This is discussed in more detail in Section 7.

5. Thrust Vector Control

The MAV TVC systems modify nozzle gimbal angles to achieve desired SRM1/SRM2 thrust vectors. It actively controls vehicle pitch and yaw during motor burns. Each stage TVC consists of a pyro-activated thermal battery, a Field Programmable Gate Array (FPGA) firmware operated controller, and two traditional electromechanical actuators clocked 90 degrees apart. The battery and controller mount to the aft dome exterior on each SRM. Actuators attach to the SRM metallic aft structures and moveable portion of the SRM nozzles. The SRM nozzle features a trapped ball design with a SSSL. Figure 9 shows the location of the first stage TVC with respect to the motor and nozzle.

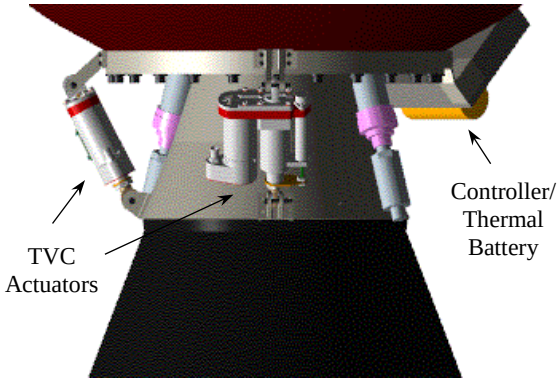

Figure 9. Stage 1 TVC

The SSSL nozzle's trapped ball design allows for vectored thrust without the need for an elastomeric gasket, as elastomeric materials have been known to become brittle in extremely cold environments. The actual joint of the nozzle is located downstream of the nozzle throat, allowing it to be unaffected by the high-pressure combustion environment. This theoretically decreases the effects of throat erosion. An example of a SSSL is shown in Figure 10.

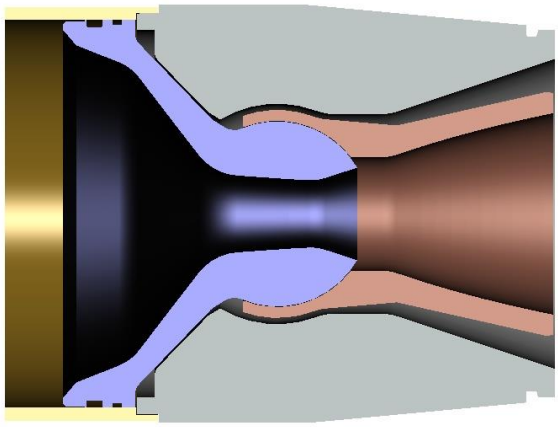

Figure 10. Example Supersonic Split Line

Thermal batteries, although extremely efficient in this application, are one-time-use power sources. Mission operations, however, call for pre-MAV flight demonstration of end-to-end TVC operation and dynamic performance prior to MAV launch. Since the power for these TVC gimbal tests cannot be provided directly by the thermal batteries, a study was performed to determine the most appropriate, alternative power source. Drawing power from the SRL would represent a nontrivial power and mass impact and would introduce a series of potential failure modes. Following the development of a test duty cycle, which would extend the full range of the gimbal angle at a maximum slew rate, it was determined that TVC gimbal testing after Earth launch should be powered entirely through the MAV power distribution board. The controller, although part of the TVC system, receives commands from the avionics flight computer.

6. STRUCTURES AND DYNAMICS

Loads & Dynamics

A structural loads analysis was performed on the integrated vehicle to ensure that it would survive the loads and environments imparted on it during various mission phases. As mentioned in Section 3, the individual SRMs contained the primary load path during EDL. The rest of the integrated vehicle, however, is still expected to undergo significant structural loads. The difference in loading hardware between propulsion and structural components are shown below in Figure 11, with orange representing structural elements and red representing propulsive elements.

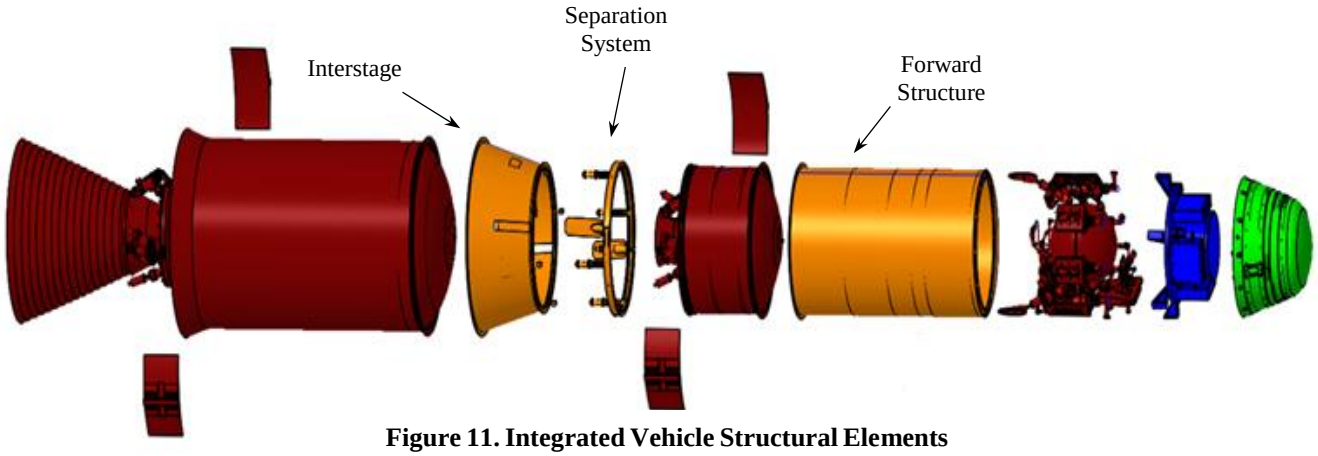

Figure 11. Integrated Vehicle Structural Elements

As mentioned earlier, the MAV loads environment is fairly atypical for a launch vehicle, in that it must endure its maximum loads in a lateral direction during EDL. To withstand this as well as axial loads during ascent, the interstage and forward structure elements were designed to be of high TRL machined monocoque construction from simple ring forgings.

The loads analysis featured three primary inputs: the 3 Degrees-of-Freedom (3DOF) trajectory, aerodynamic line loads, and a Finite Element Model (FEM) featuring a standard Craig-Bampton reduction. The FEM is shown in Figure 12. The specific loads assessed included Earth launch, Mars EDL, and Mars ascent. Thrust was applied as quasi-static pressure loads at the forward and aft domes of the SRMs to account for stage stretch. A loads uncertainty factor of 1.5 was used for all events. For the Mars ascent loads analysis, nine individual flight times were considered at key points in flight. Loads environments were used as the primary input for the structural stress analysis, based upon several dynamic contributions, such as acoustics.

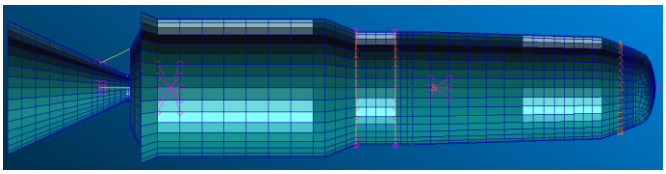

Figure 12. MAV FEM Mesh

The stress analysis itself featured single piece forging manufacturing with an optimized nominal skin thickness. The yield and ultimate Factors of Safety (FOS) were 1.25 and 1.4, respectively, per NASA-STD-5001[6]. Knockdown factors for the cylindrical forward structure and conical interstage were determined per NASA-SP-8007[7] and NASA-SP-8019[8], respectively. Only strength and buckling analyses were completed. Fracture control requirements were not imposed on the structural hardware. The structural analysis found the forward structure to have a margin of +3.06 with a yield failure mode and the interstage to have a margin of +0.46 with a buckling failure mode. The highest stress value occurred where the RCS attaches to the forward structure. The relatively low margin on the interstage introduces a risk to any increase in primary structure loads, secondary loads, access hatches additions, and changes in forging thickness/material properties. This can be mitigated in future work by designing to case-specific loads instead of maximum enveloping loads, developing robust load-carrying hatch designs, and taking advantage of material properties with regard to environmental considerations.

Mechanisms

The structural design includes all mechanisms onboard the vehicle. Although additional mechanisms may be considered in future analyses, two primary types of mechanism were

considered for DAC-0.0: stage separation hardware and pyrotechnic mechanisms. For the stage separation mechanism, a system similar to the Wallops Flight Facility clamp band was assumed. This design has flown on many sounding rockets in the past and is considered mid-to-high TRL. The system as-is has been tested to mechanical load levels that envelop expected MAV loads and can be easily adapted as the vehicle design changes in future design cycles. An image of a sample clamp band separation system is shown in Figure 13. Pyrotechnic components were used in four subsystems: the propulsion subsystem for SRM ignition, the TVC for thermal battery activation, the RCS for main isolation valve/bypass isolation valve, and the separation system for vehicle staging. The propulsion ignition system uses an Electronic Safe and Arm (ESA) assembly, manufactured by the same supplier as the SRMs. The ESA utilizes an internal semi-conductor bridge initiator to ignite combustible material interfacing with the aft end toroidal igniter of each SRM.

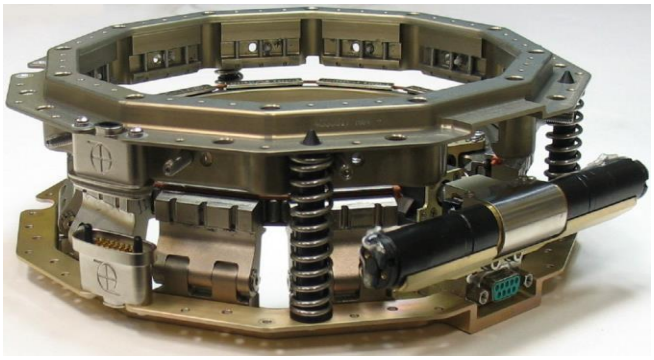

Figure 13. Sample Clamp-Based Separation System

The two pyro valves for the RCS feature high TRL metal components, selected for extremely low leakage rate, low mass, reliability, flight heritage, and versatility in customization. The clamp band separation system features four arc segments adjoined with hinges and pins at two locations. A pressure cartridge-based bolt cutter is interfaced with the fasteners to enable vehicle stage separation.

Vibration, Internal Acoustic, and Shock Environments

Part of the DAC-0.0 structural analysis included an assessment of vibration, internal acoustics, and shock environments. The random vibration analysis determined the Mars acoustically-induced and mechanically-induced random vibration Maximum Predicted Environment (MPE) for components. This featured an initial use of PAA ascent environments updated for DAC-0.0 3DOF trajectories and an updated liftoff acoustics environment via independent CFD analysis. This CFD analysis is discussed in more detail in Section 9. For the actual vehicle material, a scaled Saturn V aluminum honeycomb was used as a reference with a STAR48 SRM for motor induced vibration. These were ultimately combined to create the MPE shown in Figure 14.

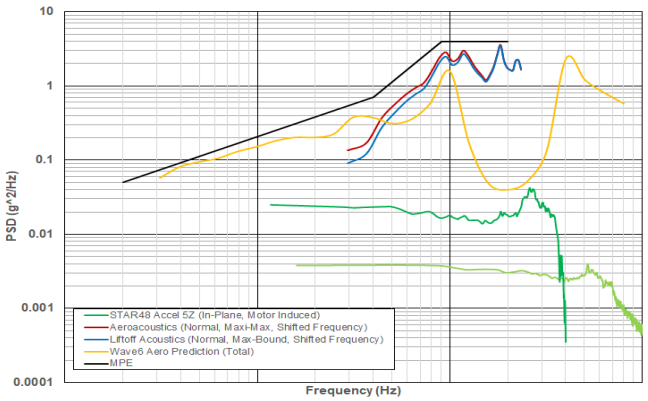

Figure 14. Random Vibration MPE

The internal acoustics analysis also used PAA environments updated for the DAC-0.0 3DOF trajectory. They were, however, applied to aeroacoustics. Empirical analysis was based upon Saturn vehicle noise reduction databases[9]. The internal acoustic Sound Pressure Level (SPL) MPEs for both liftoff and ascent are shown in Figure 15.

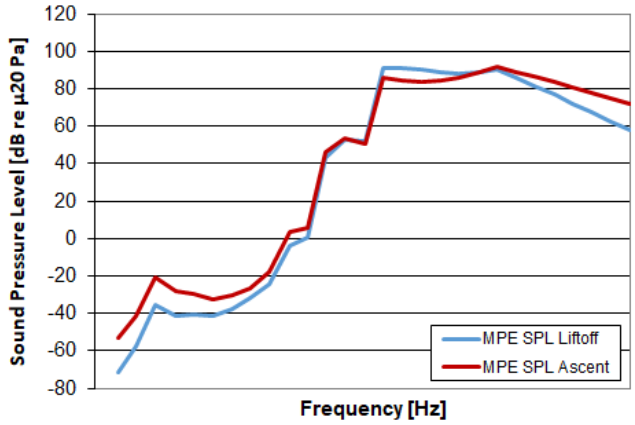

Figure 15. Internal Acoustics MPEs

The shock analysis was performed on the vehicle ascent portion of the vehicle. It determined the clampband-based stage separation to create the highest shock environment. This shock response was felt most by the RCS and avionics hardware.

7. THERMODYNAMICS

The MAV thermal environments are primarily divided into two configurations based upon different phases of the sample return mission: a non-operational configuration and an operational configuration. The non-operational configuration includes all phases of the mission in which the MAV is stowed within the SRL. During this time, the MAV is contained within a thermal enclosure, or "igloo", to help maintain a consistent external temperature and to provide an additional layer of protection against the harsh Martian environment. The MAV will be enclosed within this igloo throughout cruise to Mars, EDL, and during Mars surface operations. The MAV-SRL igloo configuration is shown in Figure 16.

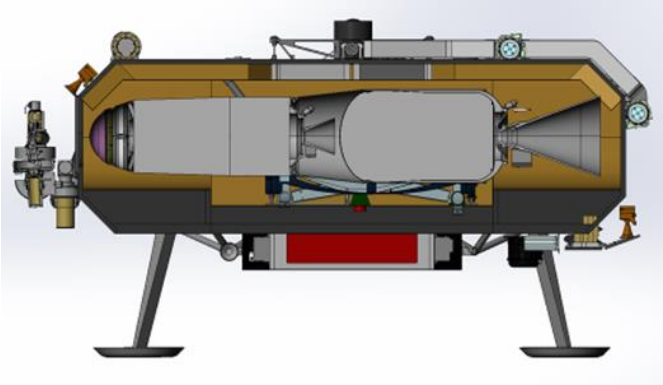

Figure 16. SRL with MAV Stowed Within Igloo

Although the integrated vehicle itself will be held at non-operational AFTs during these times, various internal components will be brought up to operational AFTs for various system checks prior to the ascent portion of the MAV mission. Once surface operations, including the transfer of sample tubes to the OS, are complete, the MAV will enter an operational phase. This configuration involves the top of the SRL opening in preparation for ejection. Additionally, this phase contains the ascent portion of the MAV mission, in which it is exposed to the Martian atmosphere and space. The prelaunch configuration of the SRL is shown in Figure 17.

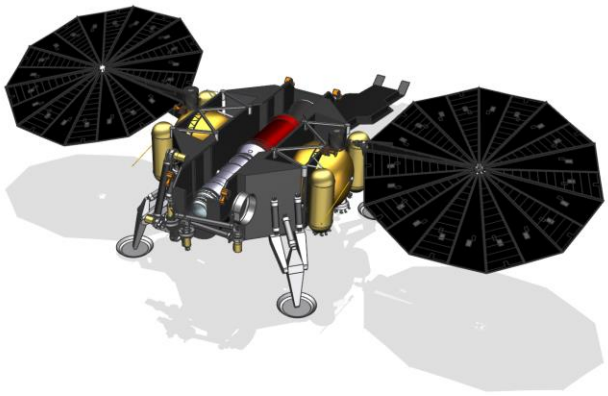

Figure 17. MAV at Operational AFT Prior to Launch

To maintain adequate AFTs during various aspects of the MAV mission lifecycle, a Thermal Control System (TCS) was developed. The TCS combines a passive and active design to maintain temperatures for all MAV solid motors, propulsion components, avionics, and structures. It consists of 16 individual heater zones for Mars surface operations and prelaunch, in addition to insulation, isolators, and thermal coatings. During this time, Platinum Resistance Thermometers (PRTs) are tied directly to the SRL computer to control and power MAV heaters. Thermal Protection System (TPS) materials were sized for Mars flight to address aerothermal and plume impingement heating to maintain MAV temperatures during ascent. The TCS and TPS were based on high TRL hardware options that have shown to be effective in Martian environments.

For the majority of the MAV mission, the vehicle will be exposed to a minimum of -62.5°C while stowed within the igloo of the SRL. During this time, the active TCS is designed to maintain an integrated vehicle AFT greater than -40°C during non-operational phases and an AFT greater than -20°C during operational phases. The 16 integrated vehicle thermal control zones of the TCS are shown in Figure 18.

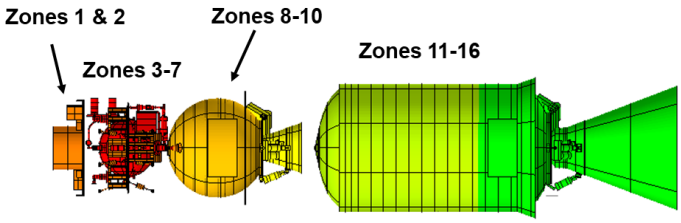

Figure 18. Integrated Vehicle Thermal Control Zones

As mentioned in Section 4, the RCS features hydrazine propellant. This presents a special case for the thermal design, as hydrazine freezes at 2°C, which is well above both operational and non-operational integrated vehicle AFTs. For this case, a special set of heaters with different performance characteristics were designed for the RCS TCS. The RCS requires a non-operational AFT greater than 14°C and an operational AFT greater than 17°C. Additionally, it features a number of added thermal control zones, shown in Figure 19.

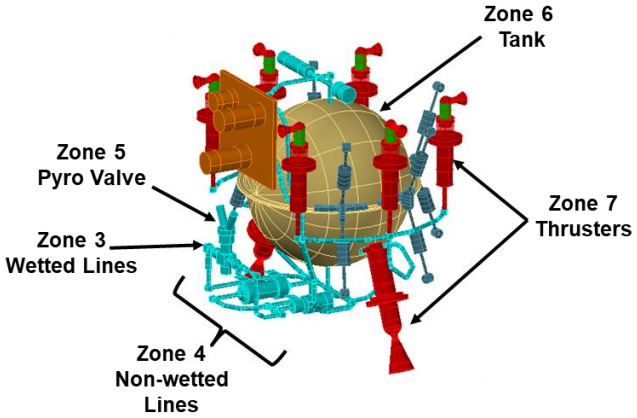

Figure 19. RCS Thermal Control Zones

During ascent, the MAV thermal performance is highly affected by the extreme Martian environment. The average Martian diurnal cycle results in the MAV experiencing thermal environments ranging from as high as approximately 10°C while on the ground to as low as -130°C during ascent. For this analysis, a worst-case solar longitude of 173° was assumed. As the MAV will only be exposed to these temperature extremes on the order of minutes, an active in-ascent flight TCS is not needed, especially after additional thermal heat sources are taken into account. The passive TPS design was developed after creating an integrated vehicle ascent heating profile. This considered aerothermodynamics and plume radiation environments, SRM nozzle and case temperatures, and TVC/avionics waste heat. The results of this analysis are shown in Figure 20 for first stage flight, with peak ascent heating temperatures occurring on the vehicle Outer Mold Line (OML) approximately 70 seconds into flight. A stagnation point was also observed at the tip of the MPA.

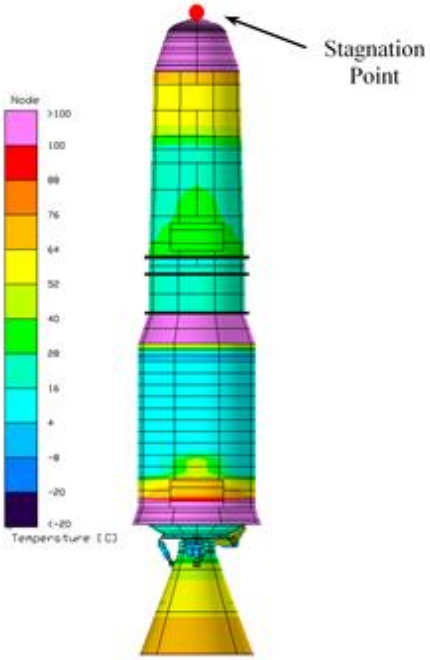

Figure 20. Peak Ascent OML Temperatures

During all MAV flight phases, an upper limit of 40°C AFT was assumed on the vehicle internal components. Figure 20 shows most of the MAV surface remains below 100°C. Higher temperatures were discovered on the MPA, interstage, and aft ramp, with the highest temperature observed on the stagnation point. Despite the areas of high temperature, the avionics hardware, RCS, SRM components, and first stage TVC components all remained below the 40°C limit. First and second stage heat soak back was not found to be a concern. The SRM2 TVC controller, however, experienced a peak temperature of approximately 118°C, exceeding the AFT upper limit. This was primarily due to plume radiation from SRM2. The SRM2 TVC controller heating will be addressed in future analysis cycles.

8. AVIONICS

The MAV avionics system is primarily responsible for three functions: command and data handling, power distribution, and communication. The hardware components include a power distribution board, RCS controller, pyro controller board, beacon, cabling, flight computer, input/output board, batteries, Inertial Measurement Unit (IMU), transmitter, and antenna. Where available, high-TRL components were used. Otherwise, components with heritage Electrical, Electronic, and Electromechanical (EEE) parts were used. The overall layout of the avionics shelf is shown in Figure 21. The avionics shelf is located in the second stage, between the RCS and MPA. Prior to first stage SRM ignition, several mission essential functions will be provided by the SRL via umbilical connections.

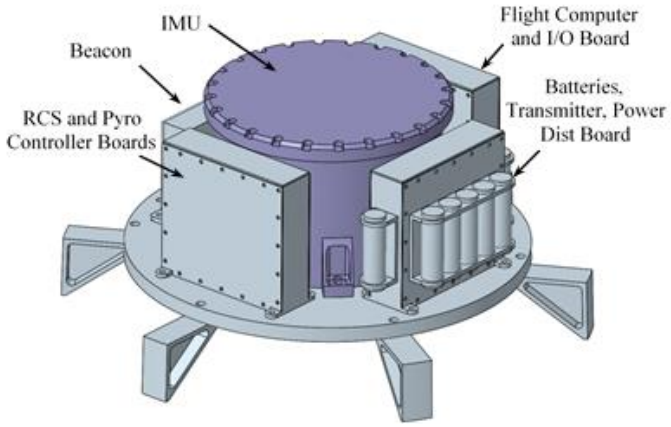

Figure 21. Avionics Hardware Layout

Command and data handling is primarily managed by the flight computer, IMU, RCS controller, and pyro board. These components allow the vehicle to sense and react to various inputs during ascent through the execution of detailed algorithms. Although the TVC controllers do receive commands from the flight computer, they are considered independent components from the avionics section. The primary computational component of the vehicle is the Sphinx flight computer. This was developed by NASA JPL for use on vehicles requiring low mass and power with radiation tolerance. For vehicle inertial measurements, the Honeywell Miniature Inertial Measurement Unit (MIMU) or similar was selected. Despite being relatively large compared to other avionics components, it has a high TRL and has proven itself to be very accurate and reliable in Martian environments. Custom RCS controller and pyro boards were added in the DAC-0.0 configuration to execute commands from the flight computer for attitude control and activation of onboard pyrotechnic mechanisms. Umbilicals from the SRL provide direct control of the active TCS of the MAV by the SRL while it is stowed. Additionally, the SRL will provide attitude and position knowledge to aid in calibration and gyrocompassing of the IMU.

For power and power distribution, onboard batteries and a custom power distribution board was developed. The power source selected for the DAC-0.0 design were LG MJ1 18650 3500mAh 10A batteries. These batteries only provide power to the MAV systems during ascent. While stowed in the SRL, power distribution umbilicals will provide power from the SRL for MAV components such as heaters and the flight computer during health and safety checks. TVC gimbal testing is a special case. Since the TVC actuators are powered during ascent by one-time-use thermal batteries, a significant amount of cabling would have been necessary to power gimbal testing from the SRL. For this reason, the onboard MAV batteries will power gimbal testing and will be recharged afterwards via power from the SRL umbilical.

The transmission of flight data such as telemetry and status will be directed to the Mars Relay Network (MRN) for relay back to Earth. This will prove vital for flight trajectory recreation and assessment. A transmitter similar to the ISIS

TRXVU was selected for this purpose due to size, capability, and compatibility with existing MRN satellites. The antenna for this transmitter will be determined in future studies. An onboard beacon also exists to serve as a navigational aid for the ERO. Following OS ejection, the beacon will activate, broadcasting a simple, periodic signal. The ERO will receive this signal and use it to determine the approximate location of the MAV and ejected OS. Despite the beacon actually being located on the MAV, it is expected that the OS will remain within close enough proximity to the spent second stage that optics aboard the ERO will be able to accurately locate the OS in relation to the MAV. The beacon is expected to remain operational for up to 25 days following activation and will have its own independent power source.

Flight Software

Although command and data handling is performed by the flight computer, the actual logic behind it lies in the flight software. The flight software is responsible for executing all flight operations and interfacing between subsystems. Each system that operates as part of the flight vehicle must have an algorithm behind it that is interpreted through flight software.

The flight software design began with identification of individual software modules that will be needed for the MAV mission. Additionally, external interfaces were identified for various hardware connections to the flight computer. The notional MAV flight software architecture for previous studies assumed a core Flight System (cFS) architecture. Although other frameworks were examined as part of the DAC-0.0 flight software design, cFS was retained due to technical capability, advantage of code and artifact reuse, developer communities, and proven flight heritage. The Real-Time Executive for Multiprocessor Systems (RTEMS) OS was selected for use on cFS.

As part of the software architecture framework decision, various software prototyping was performed to mature the design and further customize the cFS framework. This featured development of an IMU simulator; integration of early GNC code; creation of a basic navigation application; and development of a physics-based model. The final flight software system for DAC-0.0 featured three individual layers: a platform layer, a reusable layer, and a mission specific layer. The platform layer included vital code for running the flight software, such as operating system and flight computer code. The reusable layer featured standard code common to launch vehicle and spacecraft systems, such as command and telemetry and timing services. These were only slightly modified from existing cFS modules. The mission-specific layer was exclusive to the MAV design, featuring initial code for modules such as mechanism operation, GNC algorithms, and communication with MSR elements. These will be updated throughout the project lifecycle.

9. AEROSCIENCES

Although the atmosphere of Mars is significantly thinner than that of Earth, it is still dense enough for aeroscience considerations. Analyses were completed to assess the vehicle response to various aerodynamic and acoustic environments. Understanding these induced environments is vital to ensuring that vehicle hardware components will perform as expected during the mission.

Aerodynamics

Aerodynamic analysis of the vehicle began with an assessment of the vehicle shape. Vehicle OML and protuberances are the primary driving factors behind the pressure environments that ultimately determine aerodynamic performance and stability. Initially, a Missile DatCom Aerodynamic Database was used to empirically model the vehicle based upon key geometric breakpoints. This allowed the development of a preliminary aerodynamic database for use in initial GNC studies as well as pressure distribution across the vehicle at various stages in flight. These GNC studies are discussed further in Section 10. Figure 22 shows an example of the pressure coefficient across the vehicle surface.

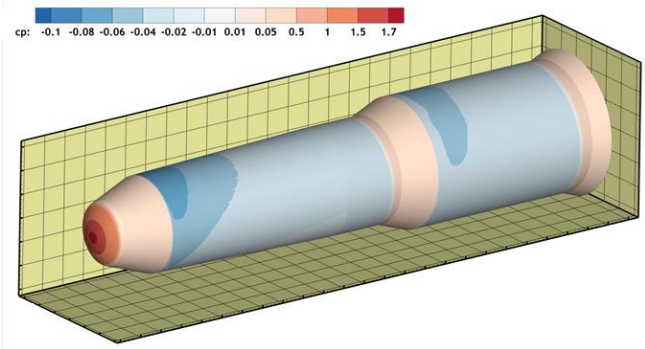

Figure 22. Vehicle Pressure Distribution

As this empirical approach was based upon an existing database, it could only provide data to a certain level of fidelity. Missile DatCom results are extremely sensitive to settings, and small vehicle features can have large ramifications on results. To check against Missile DatCom and develop higher fidelity aerodynamic coefficients, a series of CFD-based analyses were performed using the FUN3D suite of tools. An unexpected disagreement was found between Missile DatCom and FUN3D, with the CFD assessment predicting significantly lower drag across the ascent trajectory of the vehicle, at significantly lower transonic and supersonic conditions. Both methods, however, predicted the vehicle to be statically unstable across most of the trajectory, with CFD results predicting higher instability. It should be noted, however, that aerodynamic instability does not necessarily mean that the vehicle is uncontrollable. A stability comparison is shown in Figure 23 for two points on the vehicle, displaying pitching moment ($C_{m\alpha}$) at various Mach numbers for a null angle of attack (α). This shows that the pitching moment at the nose remains negative at all Mach numbers examined, whereas aft of the nose, the pitching

moment is only marginally positive. The greatest instability is predicted at low velocities.

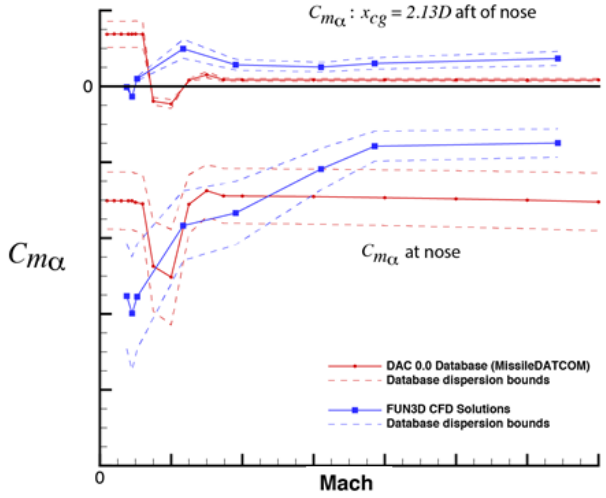

Figure 23. Aerodynamic Stability, α=0°

Further comparison between the two methods determined the CFD results to be more accurate. Comparing basic cylinder shapes confirmed matching results, indicating that the addition of physical ramps in the interstage and aft sections of the vehicle create compression shocks. These are shown in Figure 24. The pressure magnitudes and distributions are the likely source of disagreement, however, further validation will be necessary. For the development of the DAC-0.0 6DOF aerodynamic database, CFD analysis was used.

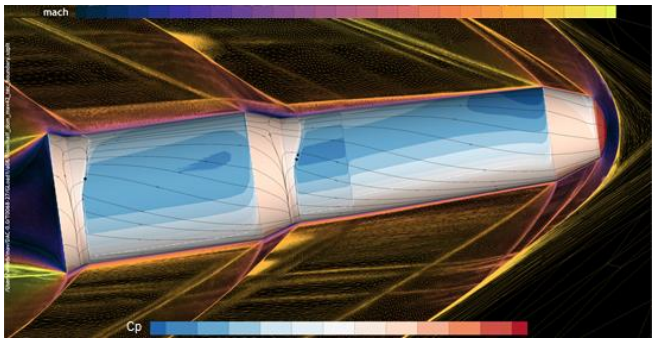

Figure 24. CFD Predicted Compression Shocks

In addition to the flow field analyses performed during DAC-0.0, an assessment was performed to determine the effect of RCS plume interactions with the vehicle aerodynamic environment. A representative CFD model was developed for the MR-111C thruster nozzles based upon available specifications. One-dimensional nozzle equations were used to estimate chamber, throat, and exit conditions to set up CFD solutions, assuming nominal thrust and neglecting scarf effects. Preliminary cases were run at MECO conditions, where stage 1 velocity would be highest, at approximately Mach 13. During stage 2 and orbital trim burns, the vehicle would be removed enough from the atmosphere to where RCS interactions with aerodynamics would not be a concern. At these conditions, it was found that RCS plumes stagnate the flow ahead of nozzles and disrupt flow downstream. The pitch RCS thrusters resulted in a net high-pressure region ahead of the vehicle CG, ultimately resulting in a positive augmentation of the RCS control authority. Examining different variations in vehicle and nozzle attitudes found that nozzle interactions created an increased commanded torque ranging between 4-40%. Although this does imply that a net decrease in RCS propellant may be feasible in future designs, it should be noted that an overly sensitive controller logic design may react negatively to too much authority.

Aerothermodynamics

Aerothermodynamic environments were developed to determine how the vehicle external surfaces would react to high velocity flow during ascent. Although the static natural environment of Mars is relatively cold, the high pressures experienced by the vehicle during ascent generate non-trivial upper temperatures. The generated environments were ultimately helpful in determining the ascent heating profile used to design the TPS discussed in Section 7 and for general MAV thermal studies. For this analysis, heating indicators were constructed using CFD with the LAURA-5 aerothermal analysis tool. Eight body points were used to provide convective heat rates and loads across the vehicle in various ascent trajectories. As shown in Figure 25, peak heating was observed on the nose. The stagnation point mentioned in Section 7 experienced the maximum surface heat for the vehicle at approximately 55sec into flight. Despite these high aerothermodynamic environments, all internal components remained within acceptable AFTs.

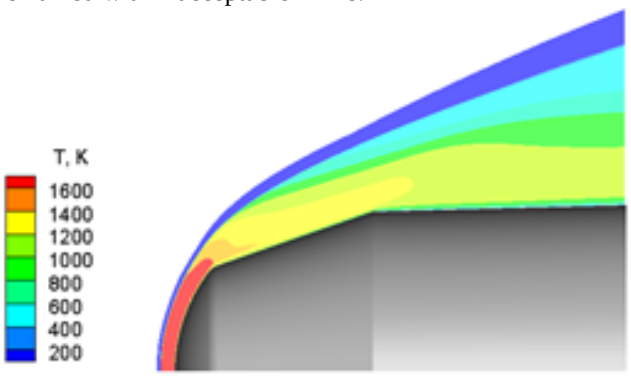

Figure 25. Nose Region Flowfield

External Acoustics

Liftoff acoustics account for the noise generated by the mixing of SRM plume exhaust flow with the surrounding atmosphere and its interactions with launch structures. SPLs were developed at five different distances from the nozzle exit plane at various one-third octave band center frequencies to assess the impact of these environments. Although higher than SPLs from previous studies, the liftoff acoustic environments were found to not present a concern for the DAC-0.0 MAV design. Similar to liftoff acoustics, plume-induced acoustics were also examined during the study. Plume-induced acoustics accounts for the noise generated by the mixing of the SRM plume exhaust flow with the mean aerodynamic flow. As with the liftoff acoustics analysis, SPLs were developed at five different distances from the nozzle exit plane at various one-third octave band center

frequencies. Once again, the plume-induced acoustic environments were found to not be a concern for the DAC-0.0 MAV design. These two acoustic environments were ultimately applied to the MAV surface loads analysis to develop design criteria for flight hardware, systems and assemblies. Ascent aeroacoustic environments account for the noise generated by aerodynamic force interactions with the vehicle surface. For this analysis, the vehicle was divided into four individual acoustic zones, shown in Figure 26.

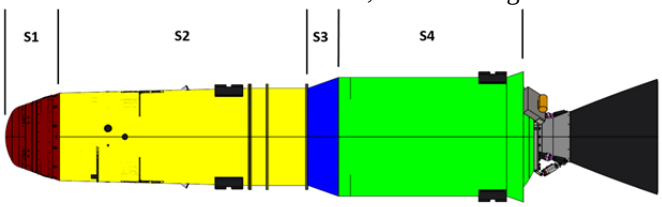

Figure 26. Ascent Aeroacoustic Zones

As with the internal acoustics analysis, the aeroacoustic analysis used PAA environments updated for the DAC-0.0 3DOF trajectory. The SPLs, shown in Figure 27, were combined with other acoustic data for use in determining the integrated vehicle loads environments. Ultimately, as with prior acoustic environments, ascent aeroacoustics were not found to be a concern for the MAV DAC-0.0 configuration. Wind tunnel testing and buffet loads analysis is planned in future cycles to add further fidelity to the aeroacoustic results.

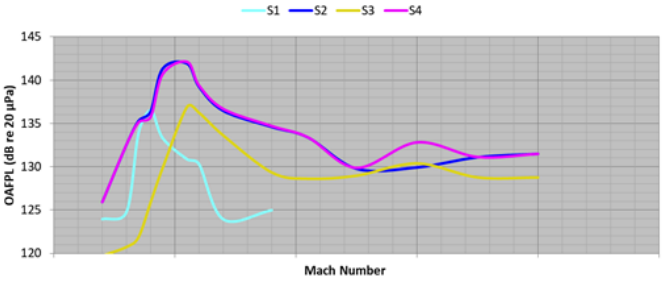

Figure 27. Ascent Aeroacoustic SPLs

10. Guidance, Navigation, & Control

Mission Analysis & Guidance

In order to successfully deliver the OS for rendezvous with the ERO, the MAV trajectory was nominally designed to target a circular orbit of 343km and an inclination angle of 27°. The TVC systems were designed for attitude control about the pitch and yaw axes during motor burns. The RCS was designed for attitude control about the roll axis during motor burns and about all axes during coast. Although a nominal trajectory can be modeled perfectly with modern computational methods using nominal parameters, the actual vehicle performance will be largely affected by uncertainties and variations of those parameters. The payload, for example, was assumed to be 16kg. The actual composition of its geological samples, however, will be of varying, immeasurable density. Additionally, some properties of the vehicle will not be known until final integrated testing has been complete. For this reason, it was necessary to develop a GNC design robust enough to handle unknown variations. Initial MAV mission analysis began with the development of a nominal 3DOF trajectory and flight plan. This was based upon preliminary mass and propulsion designs. Although a 3DOF trajectory only considers the translational motion of a point mass, it was necessary in determining how the expected payload mass would affect vehicle performance. An iterative method was used with trajectory design and propulsion parameters to determine a vehicle thrust profile and propellant flow rates. These in turn were used in sizing the solid motors. Following the development of a 3DOF trajectory, an updated list of component masses and mass properties was developed from other subsystem designs. This was combined with the 6DOF aerodynamic database described in Section 9 to design a nominal 6DOF trajectory. This took into account vehicle geometry and mass distributions to determine vehicle body rates as well as translational motion. The 6DOF analysis was instrumental in determining the capability of the TVC and RCS in terms of vehicle controllability.

Figure 28 describes the overall vehicle flight plan. This features the first stage burn being subdivided into an open-loop guidance phase and a closed-loop guidance phase. In this vehicle design, large orbital dispersions were found to accumulate during first stage open-loop guidance. The closed-loop portion helped to mitigate these dispersions. Following the nulling of any aerodynamic angles, the vehicle will enter a closed-loop attitude hold for the majority of coast. Prior to SRM2 ignition, the RCS will command the vehicle to rotate for MPA fairing separation and first stage separation before re-orienting the vehicle back into its flight vector. An energy management maneuver will then be employed by the guidance system to determine the most efficient time for SRM2 ignition. This will reduce the amount of orbit overshoot in the case of an over-performing first stage. Following a relatively short SRM2 burn to circularize the orbit, the vehicle will enter another attitude hold in order to prepare for the orbit trim burn. This final burn will reduce any excessive orbit dispersions unaccounted for by the energy management maneuver and place the vehicle in the desired orbit for OS release.

The nominal 6DOF analysis found that all original design constraints were met with regard to orbit and mass. Following development of the nominal trajectory, a set of dispersed simulations were performed to determine the vehicle response to the aforementioned unknown variations. This included dispersions on values such as launch attitude, mass properties, and aerodynamic coefficients. A Monte Carlo analysis was performed to examine these dispersions with different combinations of open- and closed-loop guidance as well as orbit trim burns. This found that surprisingly, the design was robust enough with just stage 1 open-loop guidance and no need for an orbit trim burn to meet all constraints for ERO rendezvous. Several cases, however, still fell outside of the initial MAV constraint window for the semi-major axis dispersion. Adding closed loop guidance to the stage 1 burn significantly tightened these dispersions. Further adding the orbit trim burn after stage 2 burn reduced

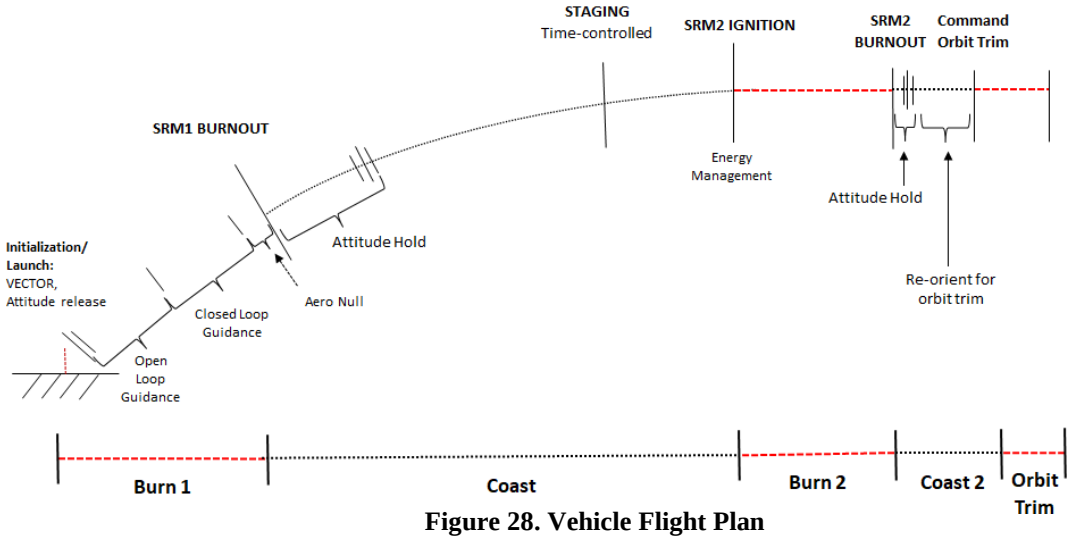

Figure 28. Vehicle Flight Plan

the dispersions even further. Ultimately, the Monte Carlo analysis found that the final vehicle configuration was able to meet all orbit constraints. Figure 29 shows a comparison of semi-major axis Monte Carlo dispersions between a stage 1 open-loop/no orbit trim scenario and a stage 1 closed-loop/orbit trim scenario, highlighting how effective the added measures were in reducing orbital dispersions.

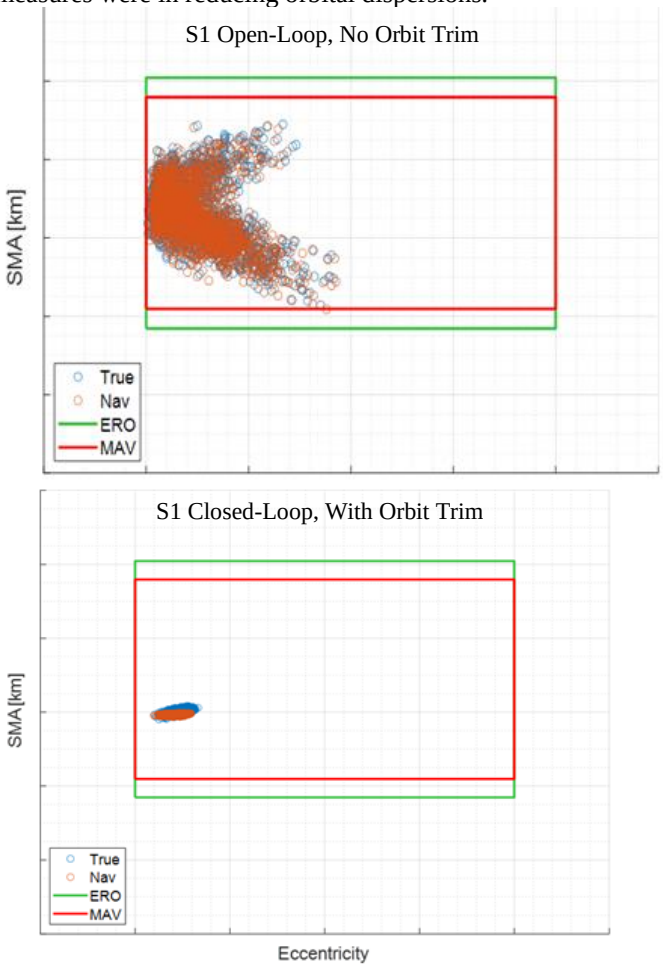

Figure 29. Guidance Effects on Orbital Dispersions

As part of the mission analysis effort for DAC-0.0, an assessment was performed to simulate stage separation dynamics. Two different separation schemes were used to provide the relative difference in velocity between the vehicle's spent first stage and primed second stage. These schemes included traditional separation springs as the baseline method as well as using OTTs as a potential mass and cost savings method. Separation dynamics between the two bodies were modeled with a multi-body 6DOF simulation tool. Results from this simulation were used with vehicle integrated CAD models to calculate near-field clearance of the nested second stage nozzle hardware as it exits the interstage. A fully dispersed Monte Carlo analysis was run on the stage separation dynamics, as well as several sensitivity studies. Dispersions and sensitivities included parameters such as stage mass properties, OTT thrust vector misalignments, and attitude rates at separation. Preliminary analysis showed feasibility in using either scheme to provide the necessary separation velocity. Near-field clearance was found to be insensitive to model input dispersions for the ranges assessed. Future analyses will determine if the added RCS propellant necessary for OTT-based stage separation will allow it to replace the traditional spring-based method as the baseline stage separation method.

Navigation

The vehicle navigational sensor capability is provided by an IMU. This sensor determines the vehicle attitude and body rates during ascent and feeds them to the flight computer in order to control the vehicle. As mentioned in Section 8, a Honeywell MIMU, or similar, was assumed for this study. As Mars does not have a significant magnetic field, it was necessary to perform a gyrocompassing analysis on the IMU to ensure its capability in meeting attitude initialization and timing assumptions. Gyrocompassing is a method of determining geographical direction using planetary rotation. The gyrocompassing analysis used the MARSNAV simulation tool. The analysis featured coarse alignment with six state vectors and nine state alignment filters. Initial Monte Carlo results indicated that the IMU was capable of meeting similar 3σ attitude initialization assumptions that were used

in previous vehicle development cycles. Unlike previous cycles, however, the IMU was found to be entirely capable of achieving this without being further augmented by a star tracker. Timing analysis found that this initialization was capable within a reasonable time period of approximately 60min. Sensitivity studies were also performed on the IMU to verify results with analytical assumptions. These found that although sensor azimuth uncertainty is sensitive to gyroscopic bias, it should not be a significant concern for the capability of the IMU.

Stability & Control

A major portion of the GNC design includes analyzing the capability of the attitude control devices to ensure that they are capable of overcoming disturbances during flight while keeping the vehicle pointed in the desired direction. This involved modeling the TVC and RCS dynamics and performing a stability analysis on each.

In both the 6DOF design and stability analysis, the TVC system was modeled with a second order transfer function based upon the dynamic bandwidth and damping coefficient from the design shown in Section 5. The control method developed was a Proportional-Integral-Derivative (PID) controller, using navigational and guidance states as an input. Proportional and derivative gains were pole-placed using estimated parameters to enable constant control margins throughout flight and precise gain scheduling with peak main thrust magnitude. The TVC control scheme is shown in Figure 30.

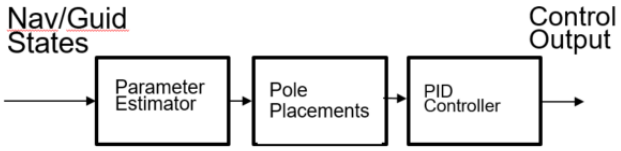

Figure 30. TVC Control Scheme

As is standard practice for this kind of analysis, stability margins for the nominal case were assumed as 6dB for gain margin and 30° for phase margin. These stability margins are measures of the vehicle's resilience to becoming unstable due to model inaccuracies and unknowns. For this vehicle, flexible body and slosh dynamics were assumed as negligible, therefore no additional margins were given for them. TVC stability margins were derived under different operating points throughout both first and second stage burns. The design demonstrated healthy margins for both gain and phase. The gain margin remained greater than 15dB at all points in flight, whereas the phase margin was fairly constant at approximately 60°. As with all launch vehicles, stability margins can diminish as the model matures. High margins such as these imply a good position for this point in the vehicle development cycle. An example of the vehicle stability margins during first stage burn is given in Figure 31. In terms of TVC controller performance, pitch and yaw attitude errors converged to within 0.1° throughout both first and second stage burns, indicating adequate tracking of commanded guidance angles. Although small transients were observed during major events such as the switch between open and closed-loop guidance in first stage burn, they were not a significant source of concern.

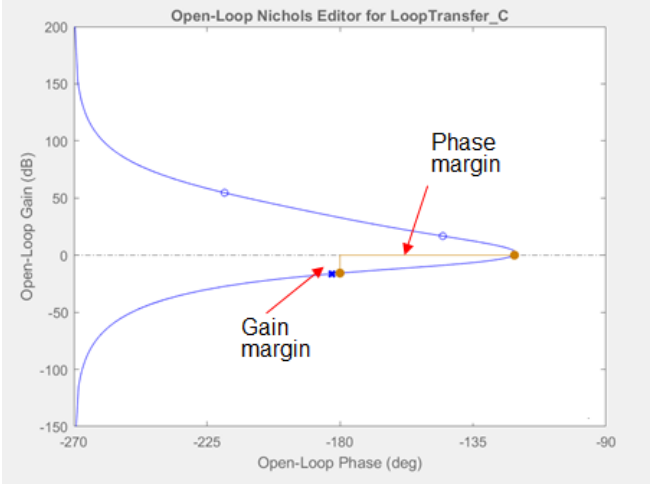

Figure 31. Sample TVC Stability Margins

For the RCS design, controllability criteria were determined through comparison of expected control torque with that of external disturbances and gyroscopic effects[11], shown in Equation 1.

$$Controllability = \frac{T_{Control}}{T_{Gyro} + T_{Dist}} \geq 2 \quad (1)$$

In addition to the controllability of the RCS, linear stability was assessed. A transfer function approximation was used, considering four variables that could affect the stability: acceleration due to control torque, deadband, rate limit, and latency. RCS controllability and stability responses were derived for six different phases of flight including first stage burn, coast phase pre-separation, coast phase post-separation, second stage burn, orbit trim coast, and orbit trim burn. Note that during main engine burn phases of ascent, RCS only provided roll control. As with TVC, at least 6dB gain margin and 30° phase margin were used to determine stability. The controllability study featured Monte Carlo analyses for each phase of flight. Except for first stage burn, all controllability results were well above the criteria established in Equation 1. As shown in Figure 32, a few Monte Carlo cases fell below the controllability factor of 2.

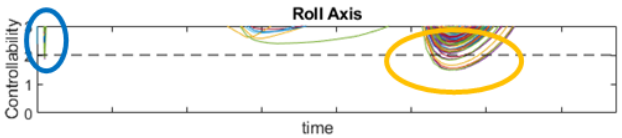

Figure 32. RCS Controllability During First Stage Burn

Despite this exceedance, the vehicle was still found to be controllable in the overwhelming majority of cases examined. Future studies will further examine sensitivities that the first stage burn may have to RCS external torques. The RCS stability analysis determined that there were large

margins for both gain and phase. In all phases of flight, gain margins remained greater than 60dB while phase margins remained greater than 50°. As with the TVC, stability margins can diminish with model maturity, so these large RCS margins provide a good position for the vehicle at this point in the development cycle.

11. Assembly, Integration, & Testing

Initial planning for AI&T of the MAV was performed during DAC-0.0. This included assembly and integration of the vehicle from subsystem components and assemblies, verification and validation testing of the integrated vehicle, and an assessment on the feasibility of an Earth-based flight test program. In support of these AI&T activities, three complete MAV units were planned: an Engineering Model (EM)/qualification unit, a Flight Test (FT) unit, and a Flight Mission (FM) unit.

The EM will be used for qualification testing of the MAV design and will be identical in hardware to the FM unit, except for having inert ordnances and pyrotechnics. Parts of this unit will also be used to support the higher-level integrated SRL Assembly, Test, and Launch Operations (ATLO) tests.

The FT unit will be used for an Earth-based flight test program. This will be done for verification and validation of the integrated MAV design. It would largely be identical to the FM unit, including live ordnances and pyrotechnics, as well as onboard development flight instrumentation. This instrumentation will be used to collect engineering data for verification and validation efforts. The FT unit will also have a flight termination system to allow range safety to terminate the vehicle's flight in case of a serious off-nominal test flight scenario.

The FM unit would be the MAV unit supporting the actual MSR mission. Sections of this unit would be combined with the EM in support of SRL's ATLO tests.

Vehicle Assembly & Integration

Planning for the assembly of the EM and the FT unit was fairly straightforward. For both units, assembly would consist of receiving and processing the major subsystem subassemblies, installing the subassemblies to primary structures, assembling the stages separately in parallel, integrating the stages into the full MAV, and then adding the MPA. Many functional checks and tests would occur throughout the phases of integration to verify workmanship of the assembly.

Initially, the FM unit was also planned to follow the same integration flow. Although this would satisfy the MAV project needs, the SRL team expressed specific needs for a MAV unit to support SRL ATLO testing. This unit must contain the actual flight mission avionics hardware and, ideally, as much of the other flight mission hardware as possible. It must also not contain any live ordnances or pyrotechnics due to the SRL team's inability to handle them in ATLO test facilities. In order to satisfy this requirement, the assembly and integration of the FM unit was re-planned to be assembled into a hybrid MAV configuration. This hybrid would be comprised of both FM unit hardware and the EM's inert motors. It would then be sent to the SRL team to support ATLO testing. After completion of ATLO testing, the hybrid model would be released back to the MAV team. The inert motors would then be replaced with the live flight mission motors to produce the final form of the integrated flight mission MAV unit.

Figure 33 visually depicts the coupled nature of the assembly and integration process for both the engineering model and the flight mission unit. Note that for the illustration, the engineering model unit is represented in green as the MAV-EM, the flight mission unit is represented in blue as the MAV-FM, and the hybrid composition is represented in tan as the MAV-ATLO.

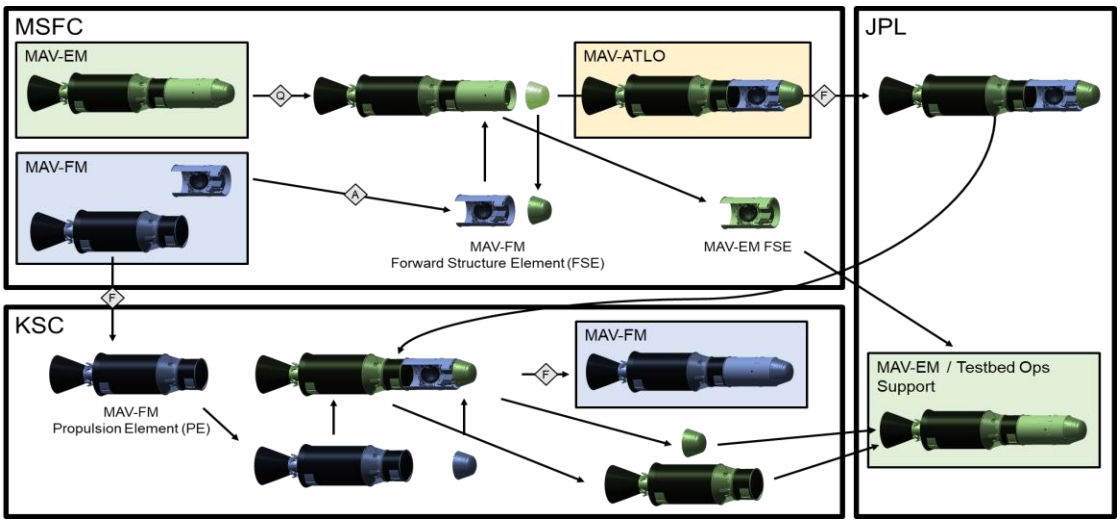

Figure 33. Notional Assembly and Integration Process for MAV EM Model & FM Units

Vehicle Testing

During DAC-0.0, planning for vehicle testing was also notionally established. In the future, all subsystem subassembly designs are expected to undergo their own qualification programs, including some hardware in the loop testing. For the avionics and flight software, a System Integration Lab (SIL) is planned to allow for software and avionics validation testing. Such a SIL was built for the Space Launch System (SLS) avionics, as shown in Figure 34.

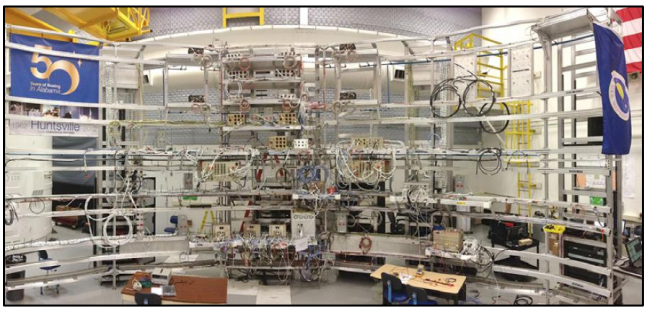

Figure 34. Example Avionics SIL (SLS)

A TVC Lab was also planned for TVC verification and validation testing, which would include a TVC controller, four actuators, a thermal battery emulator, and a two-axis active load emulator. Such a TVC Lab built for SLS is shown in Figure 35.

Figure 35. Example TVC Lab (SLS)

Subassembly hardware to be delivered for MAV unit integration would first undergo subassembly acceptance testing. Throughout integration and assembly of the MAV units, functional checks will be performed to ensure quality of workmanship during the integration of the subassemblies into the integrated MAV. The engineering model unit would undergo integrated vehicle environmental qualification testing to include thermal vacuum/cycling, leak, proof, vibration, shock, and EMI/EMC. For the FT and FM units, acceptance-level testing would be conducted for the forward structure element only, which consists of the forward structure, RCS, and avionics. These acceptance tests were planned to include thermal vacuum, leak, and proof testing only. The reason for this limitation of testing is because these two units contain live propellants that should not be subjected to a full battery of environmental testing, even at acceptance-levels. This is due to safety concerns and impacts to component life for the flight mission. Figure 36 summarizes the type of tests planned for the subsystems/subassemblies as well as for the integrated MAV units.

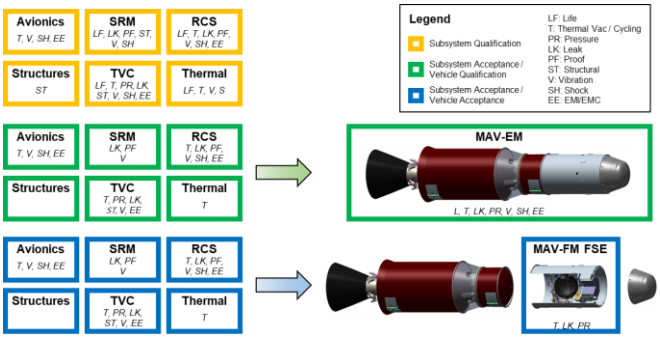

Figure 36. Summary of Subsystem and Vehicle Testing

Flight Test Planning

Given the novelty of the campaign and the uniqueness of the MAV mission in particular, an Earth-based flight test may be appropriate in order to validate the integrated MAV design. As part of DAC-0.0, the MAV team studied the feasibility with performing such a flight test, and whether it would be technically and programmatically viable.

The concept for the flight test would include the use of a high-altitude balloon with an attached MAV carrier. This system would lift the MAV to an altitude where the atmospheric pressure is similar to that on the Martian surface: approximately 30km above sea level. There, the carrier would be commanded to drop-release the MAV, at which point the MAV would begin its flight. Upon completion of its suborbital flight, the MAV stages would reenter the atmosphere and impact the ocean. The individual stages would not be recovered. The flight test concept is illustrated in Figure 37.

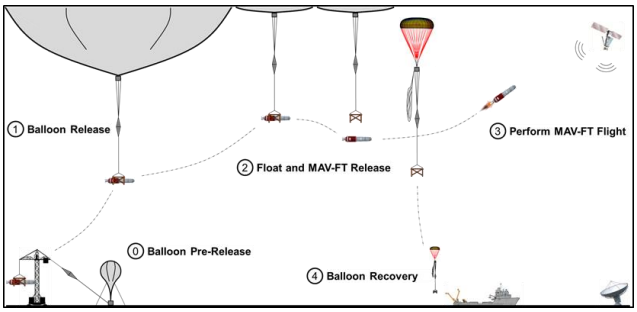

Figure 37. Notional Earth-Based MAV Test Flight

Although unconventional, a somewhat similar test program was performed by the Low-Density Supersonic Decelerator (LDSD) program, led by NASA JPL. Several domestic-based or owned test ranges and high-altitude balloon providers were informally solicited as part of this preliminary assessment. It was determined that such a test flight would be technically feasible and compatible with the current MAV project

schedule. Significant costs, however, were identified as being associated with a test flight program. A higher fidelity cost vs. benefits analysis will be necessary in the future.

12. SUMMARY

The DAC-0.0 configuration of MAV was found to successfully deliver a 16kg payload of 30 sample tubes to Martian orbit. The mission design constraints for both size and weight were met under nominal conditions. The target orbit was achieved with most 6DOF dispersions, however some cases were found to exceed the design constraint limits in various subsystems. These exceedances were minor and were not considered an area of concern. As the vehicle is still relatively early in development, future analysis cycles are expected to resolve these issues and add maturity to the design. Following the conclusion of the DAC-0.0 study, the MSR campaign identified a need for an increase in mass and volume margins aboard the SRL by reducing the mass and volume allocations given its payloads, including MAV. Future studies will examine options for further reductions to MAV mass and size, such as changing the vehicle architecture to an unguided, spin-stabilized second stage. In this alternate concept, a significant portion of avionics and RCS subsystem hardware and mass would be moved to the first stage, thus reducing total GLOM at the expense of target orbit insertion robustness and accuracy.

13. ACKNOWLEDGEMENTS

The authors would like to thank the entire MAV team for their ongoing dedication and work to the MAV project through DAC-0.0 and beyond.

14. REFERENCES

[1] D. Yaghoubi, A. Schnell, "Mars Ascent Vehicle Solid Propulsion Configuration," *IEEE Aerospace Conference, March 2020*

[2] D. Yaghoubi, A. Schnell, "Mars Ascent Vehicle Hybrid Propulsion Configuration," *IEEE Aerospace Conference, March 2020*

[3] NASA Procedural Requirements (NPR) 8704.1

[4] Aerotherm Corporation. Aerothermal Chemical Equilibrium Program (ACE), Mountain View, CA, 1969

[5] Insulation Thermal and Ablation Code, ITRAC Version 1.0, ATK Space Systems

[6] Structural Design and Test Factors of Safety for Spaceflight Hardware, NASA-STD-5001, 1996.

[7] Buckling of Thin-Walled Circular Cylinders, NASA SP-8007, 1965.

[8] Buckling of Thing-Walled Truncated Cones, NASA SP-8019, 1968.

[9] Noise Reduction Data Banks Based on Saturn V and Saturn 1B Flight Vehicles, J.R. Alexander and K.H. Reilmann, Summary Report ASD-ASTN-1792, Teledyne Brown Engineering, January 1974.

[10] Aerojet Rocketdyne In-Space Propulsion Datasheets: Monopropellant and Bipropellant Engines, April 2020. https://www.rocket.com/sites/default/files/documents/In-Space%20Data%20Sheets%204.8.20.pdf

[11] R. Hall, S. Hough, C. Orphee, K. Clements, "Design and Stability of an On-Orbit Attitude Control System Using Reaction Control Thrusters," *AIAA Guidance, Navigation, and Control Conference, January 2016*

15. BIOGRAPHY

Darius Yaghoubi *received a B.S. in Aerospace Engineering from North Carolina State University in Raleigh, NC in 2007. He has worked at NASA MSFC for 14 years. He has been a member of the MAV team since February 2018, initially starting as the GNC lead and transitioning to the vehicle technical lead in October 2018. He now works as the MAV Alternate Lead Systems Engineer. Prior to joining the MAV team, he worked as the lead pogo stability analyst on the NASA SLS program and supported separation and liftoff analysis on the NASA Ares program. He has also supported NASA groups in loads and dynamics, software integration, engineering testing, 3D printing, and deep space habitat. Aside from his technical work, Darius is an active member of the MSFC Speaker's Bureau and has represented NASA at a number of public outreach and speaking events.*

Peter Ma *is an aerospace systems engineer at NASA MSFC, serving as the MAV Project's Lead Systems Engineer (LSE) since February 2020. He has supported MAV since June 2019 initially as the assembly, integration, and test lead. He has 13 years of experience at NASA MSFC. Prior to supporting MAV, Peter served as the LSE to the Additive Manufacturing Demonstrator Engine Project and hot-fire testing. He also served as the LSE and Deputy LSE for the Aero-M Small Unmanned Aerial Systems Project and the NASA SLS Stages Project, respectively. Peter also served as the mass properties lead for the SLS Stages Project and the DOD/NASA collaborative Soldier-Warfighter Operationally Responsive Deployer for Space Program. Peter received a B.S. in Aerospace Engineering from the University of Florida in 2008.*